Frequency domain identification for multivariable motion control systems

Applied to a prototype wafer stage

Van Der Hulst, M.; González, R. A.; Classens, K.; Tacx, P.; Dirkx, N.; Van De Wijdeven, J.; Oomen, T.

DOI
10.1016/j.ifacol.2025.10.141

Publication date
2025

Document Version
Final published version

Published in
IFAC-PapersOnline

Available online at www.sciencedirect.com

ScienceDirect

IFAC PapersOnLine CONFERENCE PAPER ARCHIVE

IFAC PapersOnLine 59-17 (2025) 67–72

Frequency domain identification for multivariable motion control systems: Applied to a prototype wafer stage

M. van der Hulst * **R. A. González** * **K. Classens** * **P. Tacx** *
N. Dirkx ** **J. van de Wijdeven** ** **T. Oomen** *,***

* *Dept. of Mechanical Engineering, Eindhoven University of Technology, The Netherlands*
** *ASML, Veldhoven, The Netherlands*
*** *Delft Center for Systems and Control, Delft University of Technology The Netherlands*

Abstract: Multivariable parametric models are essential for optimizing the performance of high-tech systems. The main objective of this paper is to develop an identification strategy that provides accurate parametric models for complex multivariable systems. To achieve this, an additive model structure is adopted, offering advantages over traditional black-box model structures when considering physical systems. The introduced method minimizes a weighted least-squares criterion and uses a refined instrumental variable method to solve the estimation problem, achieving local optimality upon convergence. Experimental validation is conducted on a prototype wafer-stage system, featuring a large number of spatially distributed actuators and sensors and exhibiting complex flexible dynamic behavior, to demonstrate the effectiveness of the proposed method.

Keywords: Parameter estimation, system identification, multivariable systems, frequency response function

1. INTRODUCTION

System identification involves developing mathematical models using experimental data, often incorporating insights from physical principles (Ljung, 1999). Data-driven parametric models of multi-input multi-output (MIMO) systems are essential for optimizing the performance of engineered systems, as they enable the design of high-performance controllers and observers, provide design validation and feedback, and facilitate online monitoring and fault diagnosis (Steinbuch et al., 2022).

Traditional linear system identification approaches for multivariable systems often rely on black-box model structures that do not consider the underlying structure of the physical system. Examples include rational common denominator models and matrix fractional descriptions (Pintelon and Schoukens, 2012). The literature on these model parameterizations is extensive (Correa and Glover, 1984; Vayssettes et al., 2016), yet they may not provide the most parsimonious or physically relevant model descriptions for practical applications. Many physical systems are more naturally described by a sum of low-order transfer functions. Examples can be found in vibrational analysis (Vayssettes and Mercère, 2015; Dorosti et al., 2018) and in the control of flexible motion systems (Voorhoeve et al., 2021; Tacx et al., 2024), where models are often represented as a sum of transfer functions with distinct denominators, corresponding to the individual resonant modes of the system (Gawronski, 2004). Similar approaches are found in the thermal analysis of machine frames (Zhu et al., 2008), RLC circuits (Lange and Leone, 2021), and acoustic modeling of room responses (Jian et al., 2022). The estimation of additive transfer function models, which are related to unfactored transfer functions via partial fraction expansion, offers several advantages. These models enable more efficient parameterization by minimizing the number of parameters needed to represent the system, thereby reducing model complexity and enhancing statistical estimation properties (Söderström and Stoica, 2001). Furthermore, they provide improved physical insight for fault diagnosis (Classens et al., 2022) and enhance numerical conditioning, which is crucial for the parametric identification of stiff and high-order systems (Gilson et al., 2018).

When identifying physical systems, estimating continuous-time models offers distinct advantages over discrete-time models. Continuous-time models facilitate the integration of *a priori* knowledge, such as relative degree, and provide more interpretable parameters that directly correspond to physical quantities (Garnier, 2015). In this context, the frequency-domain approach for parametric identification of continuous-time models has become increasingly popular. Frequency-domain system identification offers several advantages, including data and computational efficiency, flexible data processing, nonparametric noise model estimation, and direct interpretation of system dynamics (Pintelon and Schoukens, 2012).

⋆ This project is funded by Holland High Tech — TKI HSTM via the PPP Innovation Scheme (PPP-I) for public-private partnerships.

10.1016/j.ifacol.2025.10.141

Many MIMO frequency-domain identification strategies have been developed for models parameterized using non-additive structures. These methods can largely be categorized into pseudo-linear regression-based techniques (Blom and Van Den Hof, 2010; Sanathanan and Koerner, 1961) and gradient descent methods (Bayard, 1994). In contrast, additive model estimation has primarily focused on single-input single-output (SISO) approaches. Examples include vector fitting (Semlyen, 1999), which involves fitting first-order pole models, a simplified refined instrumental variable method (SRIVC) for additive systems in (González et al., 2024; Young and Jakeman, 1980), and a block coordinate descent method for offline and online estimation (González et al., 2023; Classens et al., 2024).

Although additive identification offers benefits for modeling physical systems, identification methods for MIMO systems in additive structures remain limited. The approach in González et al. (2024) enables the estimation of SISO additive systems using time-domain data but is not directly applicable to MIMO systems. This paper introduces a comprehensive MIMO frequency-domain identification method for estimating additive linear continuous-time models. The main contributions are:

- C1 A frequency-domain refined instrumental variable method for estimating continuous-time MIMO models in additive transfer function form.
- C2 Experimental validation of the developed identification on a prototype wafer-stage system.

This paper is organized as follows. First, Section 2 formally introduces the additive model structure and outlines the identification problem considered. In section 3, the identification strategy is presented with experimental validation in Section 4. Finally, conclusions are given in Section 5.

Notation: Scalars, vectors and matrices are written as x, $\mathbf{x}$ and $\mathbf{X}$, respectively. The imaginary unit is denoted by $j^2 = -1$, and for $\mathbf{z} \in \mathbb{C}^n$, the operation $\Re\{\mathbf{z}\}$ returns the real part of the complex vector $\mathbf{z}$. For a matrix $\mathbf{A}$, its transpose is written as $\mathbf{A}^\top$, and its Hermitian (conjugate transpose) as $\mathbf{A}^\mathsf{H}$. If $\mathbf{x} \in \mathbb{C}^n$ and $\mathbf{Q} \in \mathbb{C}^{n\times n}$ is a Hermitian matrix, then the weighted 2-norm is given by $\|\mathbf{x}\|_\mathbf{Q} = \sqrt{\mathbf{x}^\mathsf{H}\mathbf{Q}\mathbf{x}}$. For $\mathbf{X} = [\mathbf{x}_1, \ldots, \mathbf{x}_n]$, with $\mathbf{x}_i \in \mathbb{C}^n$, the operation $\mathrm{vec}(\mathbf{X}) = [\mathbf{x}_1^\top, \ldots, \mathbf{x}_n^\top]^\top$ restructures the matrix into a vector by stacking its columns.

2. SETUP AND PROBLEM FORMULATION

In this section, the experimental setup is presented and the additive model structure is formally introduced. Finally, the identification problem considered is formulated.

2.1 Experimental setup: prototype wafer-stage system

The considered experimental setup depicted in Figure 1 is a prototype wafer stage system. The system is actively controlled in six motion degrees of freedom at a sampling rate of 10 kHz, achieving accuracy in the sub-micrometer range. The stage is magnetically levitated using gravity compensators, achieving a mid-air equilibrium and eliminating any mechanical connections to the fixed world. These systems exhibit pronounced flexible dynamics, which pose significant challenges for controller design, model updating, and monitoring techniques. The availability of accurate mathematical models that capture the dynamics of the flexible multivariable system is crucial for effectively addressing these challenges.

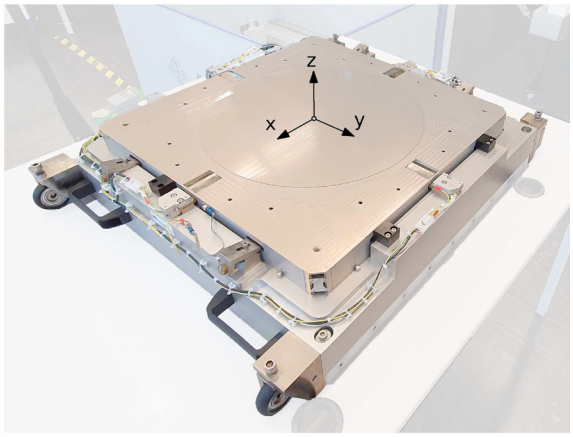

Fig. 1. Experimental setup featuring a prototype wafer-stage system.

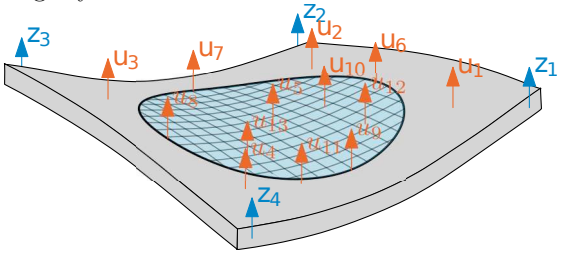

Fig. 2. Schematic overview of the featured actuators u_i and sensors z_i in the out-of-plane direction.

The system contains 17 actuators: 13 are in the z direction and two each for the x and y directions. Furthermore, the system includes 7 positioning sensors, 4 for the z-direction, 2 for the x-directions, and a single sensor for the y-direction. Only out-of-plane motions, that is, translation along the z axis, and rotations around the x and y axes, are considered in this paper to facilitate the exposition. An overview of the sensors and actuators considered is provided in Figure 2.

2.2 Model structure

To model the input/output dynamics of the wafer-stage system, an additive model structure is adopted, which is formally introduced in this section. Consider the linear and time-invariant (LTI) model of a MIMO system with n_u inputs and n_y outputs in additive form

$$\mathbf{P}(s, \boldsymbol{\beta}) = \sum_{i=1}^{K} \mathbf{P}_i(s, \boldsymbol{\theta}_i), \tag{1}$$

with K the number of submodels, s the Laplace variable and $\boldsymbol{\beta}$ and $\boldsymbol{\theta}_i$ the joint and submodel parameter vector. Each submodel $\mathbf{P}_i(s, \boldsymbol{\theta}_i)$ is parametrized according to

$$\mathbf{P}_i(s, \boldsymbol{\beta}) = \frac{1}{s^{\ell_i} A_i(s)} \mathbf{B}_i(s), \tag{2}$$

where at most one submodel may include $\ell_i > 0$ poles at the origin. The scalar denominator polynomial $A_i(s)$ and the matrix numerator polynomial $\mathbf{B}_i(s)$ are such that

no complex number z simultaneously satisfies $A_i(z) = 0$ and $\mathbf{B}_i(z) = \mathbf{0}$. To ensure a unique characterization of $\{\mathbf{P}_i(s)\}_{i=1}^K$, it is assumed that at most one submodel $\mathbf{P}_i(s)$ is biproper. The $A_i(s)$ and $\mathbf{B}_i(s)$ polynomials are parametrized as

$$A_i(s) = 1 + a_{i,1}s + \ldots + a_{i,n_i}s^{n_i}, \tag{3}$$
$$\mathbf{B}_i(s) = \mathbf{B}_{i,0} + \mathbf{B}_{i,1}s + \ldots + \mathbf{B}_{i,m_i}s^{m_i}, \tag{4}$$

where the $A_i(s)$ polynomials are stable, i.e., all roots lie in the left-half plane, and they do not share any common roots. The polynomials $A_i(s)$ and $\mathbf{B}_i(s)$ are jointly described by the parameter vector

$$\boldsymbol{\beta} = \left[\boldsymbol{\theta}_1^\top,\ \ldots,\ \boldsymbol{\theta}_K^\top\right]^\top, \tag{5}$$

where $\boldsymbol{\theta}_i$ for $i = 1, \ldots, K$ contains the parameters of the ith submodel

$$\boldsymbol{\theta}_i = \left[a_{i,1}, \ldots, a_{i,n_i}, \operatorname{vec}(\mathbf{B}_{i,0})^\top, \ldots, \operatorname{vec}(\mathbf{B}_{i,m_i})^\top\right]^\top. \tag{6}$$

2.3 Identification problem

A dataset of noisy plant frequency response function (FRF) measurements $\mathbf{G}(\omega_k) \in \mathbb{C}^{n_\mathrm{y}\times n_\mathrm{u}}$ of length N, is assumed to be available for the estimation problem. To estimate continuous-time models from the measured FRF, the pseudo-continuous-time setting is adopted (see Wang and Garnier (2008), Chapter 8 for details). The identification problem is formulated based on the matrix residual, which is computed as the difference between the FRF measurement and the model, according to

$$\mathbf{E}(\omega_k, \boldsymbol{\beta}) = \mathbf{G}(\omega_k) - \mathbf{P}(\xi_k, \boldsymbol{\beta}), \tag{7}$$

where $\xi_k = j\omega_k$. The parameter vector estimate $\hat{\boldsymbol{\beta}}$ is obtained as the minimizer of the weighted least-squares criterion

$$\hat{\boldsymbol{\beta}} = \arg\min_{\boldsymbol{\beta}} \frac{1}{2N}\sum_{k=1}^{N} \left\|\operatorname{vec}\big(\mathbf{E}(\omega_k, \boldsymbol{\beta})\big)\right\|^2_{\mathbf{W}(\omega_k)}, \tag{8}$$

where $\mathbf{W}(\omega_k) \in \mathbb{C}^{n_\mathrm{u}n_\mathrm{y}\times n_\mathrm{u}n_\mathrm{y}}$ is a frequency-dependent weighting matrix. The problem considered is to estimate additive models as described by (1), that minimizes the cost function in (8), given a dataset of noisy FRF measurements.

3. IDENTIFICATION STRATEGY FOR ADDITIVE MIMO SYSTEMS

In this section, an iterative linear regression method is introduced to solve the nonlinear and nonconvex optimization problem (8), thereby constituting contribution C1.

3.1 Criterion for optimality

The minimizers of the cost function in (8) satisfy the first-order optimality condition

$$\mathbf{0} = \frac{1}{N}\sum_{k=1}^{N} \Re\left\{\hat{\boldsymbol{\Phi}}(\omega_k, \boldsymbol{\beta})\, \mathbf{W}(\omega_k) \operatorname{vec}\big(\mathbf{E}(\omega_k, \boldsymbol{\beta})\big)\right\}, \tag{9}$$

with the gradient

$$\hat{\boldsymbol{\Phi}}(\omega_k, \boldsymbol{\beta}) = \left(\frac{\partial \operatorname{vec}\big(\mathbf{E}(\omega_k, \boldsymbol{\beta})\big)}{\partial \boldsymbol{\beta}^\top}\right)^{\mathsf{H}}. \tag{10}$$

For the considered additive model structure the gradient corresponds to

$$\hat{\boldsymbol{\Phi}}(\omega_k, \boldsymbol{\beta}) = \left[\ \hat{\boldsymbol{\Phi}}_1^{\mathsf{H}}(\omega_k, \boldsymbol{\theta}_1)\ \ldots\ \hat{\boldsymbol{\Phi}}_K^{\mathsf{H}}(\omega_k, \boldsymbol{\theta}_K)\ \right]^{\mathsf{H}}, \tag{11}$$

where $\hat{\boldsymbol{\Phi}}_i(\omega_k, \boldsymbol{\theta}_i)$ for $i = 1, \ldots, K$ is given by

$$\hat{\boldsymbol{\Phi}}_i(\omega_k, \boldsymbol{\beta}) = \left[\frac{-\xi_k \mathbf{p}_i(\xi_k, \boldsymbol{\theta}_i)}{\xi_k^{\ell_i} A_i(\xi_k)}, \ldots, \frac{-\xi_k^{n_i} \mathbf{p}_i(\xi_k, \boldsymbol{\theta}_i)}{\xi_k^{\ell_i} A_i(\xi_k)}, \frac{\mathbf{I}_{n_\mathrm{u}n_\mathrm{y}}}{\xi_k^{\ell_i} A_i(\xi_k)}, \ldots, \frac{\xi_k^{m_i}\mathbf{I}_{n_\mathrm{u}n_\mathrm{y}}}{\xi_k^{\ell_i} A_i(\xi_k)}\right]^{\mathsf{H}}, \tag{12}$$

with $\mathbf{p}_i(\xi_k, \boldsymbol{\theta}_i) = \operatorname{vec}(\mathbf{P}_i(\xi_k, \boldsymbol{\theta}_i))$ the vectorized plant of the ith submodel. In the following subsections, the first-order optimality condition (9) will be exploited to derive an estimator for the parameter vector $\hat{\boldsymbol{\beta}}$.

3.2 Refined instrumental variables for additive systems

The condition in (9) is non-linear in the parameter vector $\boldsymbol{\beta}$. A solution is obtained by reformulating (7) to a pseudolinear form which enables the refined instrumental variables approach. For each submodule in the additive model structure, the residual can be reformulated into an unique pseudolinear regression, as stated in the following lemma.

Lemma 1. The pseudolinear regression form of the residual (7) corresponding to the ith submodel is expressed as

$$\operatorname{vec}\big(\mathbf{E}(\omega_k, \boldsymbol{\beta})\big) = \tilde{\mathbf{g}}_{f,i}(\omega_k, \boldsymbol{\beta}) - \boldsymbol{\Phi}_i^\top(\omega_k, \boldsymbol{\beta})\, \boldsymbol{\theta}_i, \tag{13}$$

with the regressor

$$\boldsymbol{\Phi}_i(\omega_k, \boldsymbol{\beta}) = \left[\frac{-\xi_k \tilde{\mathbf{g}}_i(\omega_k, \boldsymbol{\beta})}{A_i(\xi_k)}, \ldots, \frac{-\xi_k^{n_i} \tilde{\mathbf{g}}_i(\omega_k, \boldsymbol{\beta})}{A_i(\xi_k)}, \frac{\mathbf{I}_{n_\mathrm{u}n_\mathrm{y}}}{\xi^{\ell_i} A_i(\xi_k)}, \ldots, \frac{\xi_k^{m_i}\mathbf{I}_{n_\mathrm{u}n_\mathrm{y}}}{\xi_k^{\ell_i} A_i(\xi_k)}\right]^\top, \tag{14}$$

and where $\tilde{\mathbf{g}}_{f,i}(\omega_k, \boldsymbol{\beta}) = A_i^{-1}(\xi_k)\tilde{\mathbf{g}}_i(\omega_k, \boldsymbol{\beta})$ with $\tilde{\mathbf{g}}_i(\omega_k, \boldsymbol{\beta}) = \operatorname{vec}(\tilde{\mathbf{G}}_i(\omega_k, \boldsymbol{\beta}))$ the residual plant of the ith submodel, defined by

$$\tilde{\mathbf{G}}_i(\omega_k, \boldsymbol{\beta}) = \mathbf{G}(\omega_k) - \sum_{\substack{\ell=1,\ldots,K \\ \ell\neq i}} \mathbf{P}_\ell(\xi_k, \boldsymbol{\theta}_\ell). \tag{15}$$

Proof. *The residual* (7) *is rewritten for* $i = 1, \ldots, K$ *according to*

$$\mathbf{E}(\omega_k, \boldsymbol{\beta}) = \tilde{\mathbf{G}}_i(\omega_k, \boldsymbol{\beta}) - \frac{\mathbf{B}_i(\xi_k)}{\xi_k^{\ell_i} A_i(\xi_k)}, \tag{16}$$
$$= \frac{1}{\xi_k^{\ell_i} A_i(\xi_k)}\left(\xi_k^{\ell_i} A_i(\xi_k)\, \tilde{\mathbf{G}}_i(\omega_k, \boldsymbol{\beta}) - \mathbf{B}_i(\xi_k)\right), \tag{17}$$

with $\tilde{\mathbf{G}}_i$ *defined in* (15)*. Substituting the numerator and denominator polynomials* (3) *and* (4)*, and vectorizing both sides,* (17) *yields*

$$\operatorname{vec}\big(\mathbf{E}(\omega_k, \boldsymbol{\beta})\big) = \frac{\tilde{\mathbf{g}}_i(\omega_k, \boldsymbol{\beta})}{A_i(\xi_k)} + \ldots + \frac{a_{n_i}\xi_k^{n_i}\tilde{\mathbf{g}}_i(\omega_k, \boldsymbol{\beta})}{A_i(\xi_k)} - \frac{\operatorname{vec}(\mathbf{B}_{i,0})}{\xi_k^{\ell_i} A_i(\xi_k)} - \ldots - \frac{\xi_k^{m_i}\operatorname{vec}(\mathbf{B}_{i,m})}{\xi_k^{\ell_i} A_i(\xi_k)}. \tag{18}$$

This expression can directly be written in the form (13) *by considering* (6)*, thereby completing the proof.* □

The residual formulation in (13) defines K pseudolinear regressions. Introducing the stacked signals

$$\boldsymbol{\Upsilon}\left(\omega_k, \boldsymbol{\beta}\right) = \begin{bmatrix} \tilde{\mathbf{g}}_{f,1}(\omega_k, \boldsymbol{\beta}) & \dots & \tilde{\mathbf{g}}_{f,K}(\omega_k, \boldsymbol{\beta}) \end{bmatrix}^\top, \quad (19)$$

$$\boldsymbol{\Phi}\left(\omega_k, \boldsymbol{\beta}\right) = \begin{bmatrix} \boldsymbol{\Phi}_1^\top\left(\omega_k, \boldsymbol{\beta}\right) & \dots & \boldsymbol{\Phi}_K^\top\left(\omega_k, \boldsymbol{\beta}\right) \end{bmatrix}^\top, \quad (20)$$

and the parameter matrix

$$\mathcal{B} = \begin{bmatrix} \boldsymbol{\theta}_1 & & \mathbf{0} \\ & \ddots & \\ \mathbf{0} & & \boldsymbol{\theta}_K \end{bmatrix}, \quad (21)$$

which contains the elements of $\boldsymbol{\beta}$ along the block diagonal, allows to write the equivalent optimality condition (9) for the K subproblem as

$$\sum_{k=1}^{N} \Re\left\{ \hat{\boldsymbol{\Phi}}(\omega_k, \boldsymbol{\beta}) \mathbf{W}(\omega_k) \Big(\boldsymbol{\Upsilon}^\top(\omega_k, \boldsymbol{\beta}) - \boldsymbol{\Phi}^\top(\omega_k, \boldsymbol{\beta}) \mathcal{B} \Big) \right\} = \mathbf{0}. \quad (22)$$

The solution to (22) is found iteratively by fixing $\boldsymbol{\beta} = \boldsymbol{\beta}^{\langle j \rangle}$ at the jth iteration in (19), the regressor (20), and additionally the gradient (11), which leads to the following iterative procedure.

Algorithm 1. Given an initial estimate $\boldsymbol{\beta}^{\langle 0 \rangle}$ and a tolerance ϵ, compute a new estimate until $\|\boldsymbol{\beta}^{\langle j+1 \rangle} - \boldsymbol{\beta}^{\langle j \rangle}\| / \|\boldsymbol{\beta}^{\langle j \rangle}\| < \epsilon$ using:

$$\mathcal{B}^{\langle j+1 \rangle} = \left[\sum_{k=1}^{N} \hat{\boldsymbol{\Phi}}(\omega_k, \boldsymbol{\beta}^{\langle j \rangle}) \mathbf{W}(\omega_k) \boldsymbol{\Phi}^\top(\omega_k, \boldsymbol{\beta}^{\langle j \rangle}) \right]^{-1} \times \sum_{k=1}^{N} \hat{\boldsymbol{\Phi}}(\omega_k, \boldsymbol{\beta}^{\langle j \rangle}) \mathbf{W}(\omega_k) \boldsymbol{\Upsilon}^\top(\omega_k, \boldsymbol{\beta}^{\langle j \rangle}), \quad (23)$$

where the updated parameter vector $\boldsymbol{\beta}^{\langle j+1 \rangle}$ is extracted from the block-diagonal coefficients of $\mathcal{B}^{\langle j+1 \rangle}$, as described in (21).

The convergence point of the iterations described by (23) satisfies the first-order optimality condition in (9). As a result, the estimate corresponds to a stationary point of the cost function defined in (8), thereby ensuring local optimality. Since the original cost function is non-convex, accurate initialization is critical to ensure convergence to the global optimum.

Remark 1. As stability is not explicitly enforced in the estimator (23), the resulting model may contain unstable poles. A common approach to address this is to reflect any unstable continuous-time poles across the imaginary axis at each iteration (Wang and Garnier, 2008). Alternatively, if each submodel has a denominator of order $n_i \leq 2$, stability can be directly enforced by constraining the denominator coefficients to be positive.

Remark 2. Note that the iterations described by (23) correspond to a refined instrumental variable method, where $\hat{\boldsymbol{\Phi}}$ is interpreted as the instrument matrix (Young and Jakeman, 1980). Furthermore, for $K = 1$, the iterations in (23) correspond to the frequency-domain refined instrumental variable method in Blom and Van Den Hof (2010), and by replacing $\hat{\boldsymbol{\Phi}}$ with $\boldsymbol{\Phi}$ to the SK iterations by Sanathanan and Koerner (1961). The method can be considered as a MIMO frequency-domain variant of the SISO approach introduced in González et al. (2024).

3.3 Initialization

The iterations in (23) require an initial estimate $\boldsymbol{\beta}^{\langle 0 \rangle}$ of the model parameters. This section introduces a method for computing the numerator parameters assuming fixed denominator polynomials. This reduces the initialization problem to determining initial pole locations, which are often effectively obtained from the nonparametric FRF model. To this end, assume that the denominator polynomials are fixed at $\bar{A}_i(s)$, and let $\boldsymbol{\eta}$ represent the parameter vector from (5) without the denominator coefficients. The estimate $\hat{\boldsymbol{\eta}}$ is found as the solution to the convex problem

$$\hat{\boldsymbol{\eta}} = \arg\min_{\boldsymbol{\eta}} \frac{1}{2N} \sum_{k=1}^{N} \| \operatorname{vec}\big(\mathbf{G}(\omega_k)\big) - \boldsymbol{\Phi}^\top\left(\omega_k\right) \boldsymbol{\eta} \|_2^2, \quad (24)$$

where the regressor matrix $\boldsymbol{\Phi}$ is obtained by stacking for each submodel

$$\boldsymbol{\Phi}_i\left(\omega_k\right) = \begin{bmatrix} \frac{\mathbf{I}_{n_\mathrm{u} n_\mathrm{y}}}{\xi^{\ell_i} \bar{A}_i(\xi_k)}, \dots, \frac{\xi^{m_i} \mathbf{I}_{n_\mathrm{u} n_\mathrm{y}}}{\xi^{\ell_i} \bar{A}_i(\xi_k)} \end{bmatrix}^\top, \quad (25)$$

in the same way as (20). Hence, an initial estimate $\boldsymbol{\beta}^{\langle 0 \rangle}$ is determined by first providing initial pole locations, which enables the computation of the numerator parameters by solving the convex problem (24) given data.

4. EXPERIMENTAL VALIDATION

This section presents the experimental validation of the introduced identification strategy, thereby providing contribution C2. The considered system is the prototype wafer-stage system introduced in Section 2.

4.1 Model structure

The input/output dynamics of the wafer-stage system, which consists of $n_\mathrm{y} = 4$ outputs and $n_\mathrm{u} = 13$ inputs, is modeled in the additive structure

$$\mathbf{P}(s, \boldsymbol{\beta}) = \frac{\mathbf{B}_{1,0}}{s^2} + \sum_{i=2}^{n_\mathrm{flex}} \frac{\mathbf{B}_{i,0}}{s^2/\omega_i^2 + 2(\zeta_i/\omega_i)s + 1}, \quad (26)$$

where the components of the decomposition are interpreted as rigid-body modes and flexible dynamic modes, with $\omega_i > 0$ the resonance frequencies, $\zeta_i > 0$ the corresponding damping coefficients, and n_flex the number of flexible modes (Gawronski, 2004).

4.2 Nonparametric modeling

As a first step in frequency-domain identification, a nonparametric model needs to be identified. The nonparametric FRF model of the (4×13) plant, representing the out-of-plane dynamics of the wafer-stage system, is obtained using the robust best-linear approximation approach described in (Pintelon and Schoukens, 2012, Chapter 3). The experiments are performed in a closed-loop configuration since active control of the mid-air equilibrium is required for stable operation. The plant FRF is derived using the indirect method, where the system is excited by n_u single-axis random-phase multisine signals with a flat amplitude spectrum. The multi-sine excitation includes 10 periods and 10 realizations, resulting in a plant FRF consisting of $N = 4000$ complex data points spanning a frequency range of 0.25 Hz to 2000 Hz. Frequency lines below 20 Hz

are discarded during the parametric estimation step, as the coherence of the estimated FRF is of low quality at lower frequencies. The delays introduced by the hold circuit in the digital measurement environment are determined based on the FRF model. The dataset is then compensated for these delays, allowing the delay-corrected FRF to be modeled in continuous time (Wang and Garnier, 2008, Chapter 8).

4.3 Weighting filter design

For the weighting filter an element-wise inverse plant magnitude weighting is selected, given by

$$\mathbf{W}(\omega_k) = \operatorname{diag}\Big(\operatorname{vec}\left(|\mathbf{G}(\omega_k)|\right)\Big)^{-1}. \tag{27}$$

The inverse plant magnitude weighting effectively transforms the matrix residual (7) from absolute to relative error criterion. This prevents overemphasizing frequencies with a large magnitude, which can dominate the estimation process, especially for systems containing integrator dynamics.

4.4 Initialization and model order selection

Due to the non-convexity of the cost function in (8), accurate initialization of the estimator in (23) is essential. The initialization approach followed is to first derive initial pole locations using the Complex Mode Indicator Function (CMIF) (Shih et al., 1988), which are then used to initialize the numerator parameters via (24). The CMIF is computed as the squared singular values of the FRF matrix at each frequency point, with the number of flexible modes n_{flex} and their corresponding frequencies determined by the peak locations in the CMIF.

Figure 3 shows the CMIF of the FRF dataset. Using this approach, $n_{\text{flex}} = 17$ distinct flexible modes are identified in the dataset. The frequency locations of the peaks in the CMIF are used to initialize the natural frequencies ω_i. The corresponding damping coefficients are initialized as $\zeta_i = 0.01$ for $i = 1, \ldots, n_{\text{flex}}$, which is a typical value encountered for lightly-damped systems. The initial modal parameters determine the pole locations, which in turn allow the initial estimates of the numerator parameters to be computed by solving the convex problem (24).

4.5 Results

The parametric model is estimated through 10 iterations of (23). The frequency response of the estimated plant model is shown in Figure 4, along with the FRF model used as data. Additionally, Figure 5 presents the frequency response of a single plant entry, together with the corresponding residual. The parametric model closely aligns with the FRF measurement across the entire frequency range, demonstrating the validity of the proposed method. In particular, the high-frequency flexible modes are accurately captured by the additive structure, which is often challenging to achieve using traditional model structures.

5. CONCLUSION

This paper addresses the parametric identification of multivariable systems using frequency-domain datasets. The introduced method, which uses a refined instrumental variable method to minimize a least-squares criterion, enables direct estimation of additive transfer function models. Many systems are more naturally described in an additive structure, leading to reduced complexity models, improved conditioning, and enhanced physical insight. The procedure has been successfully tested on a prototype wafer-stage system, providing accurate models over a large frequency range.

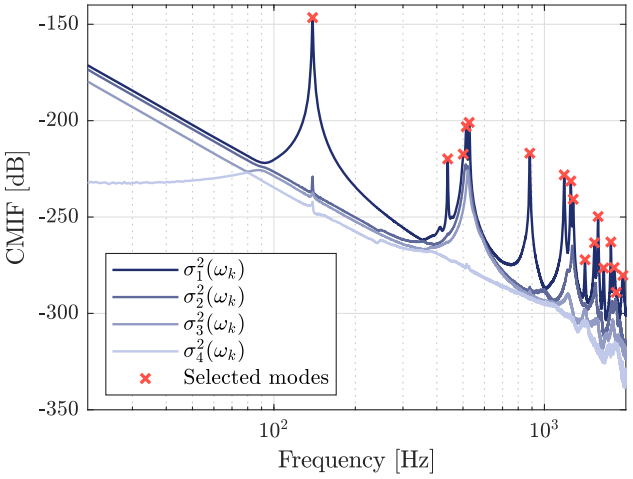

Fig. 3. CMIF plot with $\sigma_i(\omega_k)$ the ith singular value of the measured FRF dataset. The frequency locations of the flexible modes are indicated by peaks in the singular value plot. This information is used to determine the number of modes and provides accurate initial estimates of the corresponding natural frequency.

REFERENCES

Bayard, D.S. (1994). High-order multivariable transfer function curve fitting: Algorithms, sparse matrix methods and experimental results. *Automatica*, 30(9), 1439–1444.

Blom, R.S. and Van Den Hof, P. (2010). Multivariable frequency domain identification using IV-based linear regression. In *Proceedings of the IEEE Conference on Decision and Control*, 1148–1153.

Classens, K., González, R.A., and Oomen, T. (2024). Recursive Identification of Structured Systems: An Instrumental-Variable Approach Applied to Mechanical Systems. *Submitted for journal publication.*

Classens, K., Mostard, M., Van De Wijdeven, J., W.P.M.H. Heemels, and Oomen, T. (2022). Fault Detection for Precision Mechatronics: Online Estimation of Mechanical Resonances. In *IFAC-PapersOnLine*, volume 55, 746–751. Elsevier B.V.

Correa, G.O. and Glover, K. (1984). Pseudo-canonical Forms, Identifiable Parametrizations and Simple Parameter Estimation for Linear Multivariable Systems: Input-Output Models. *Automatica*, 20(4), 429–442.

Dorosti, M., Fey, R.H., Heertjes, M.F., and Nijmeijer, H. (2018). Iterative Pole–Zero model updating: A combined sensitivity approach. *Control Engineering Practice*, 71, 164–174.

Garnier, H. (2015). Direct continuous-time approaches to system identification. Overview and benefits for practical applications. In *European Journal of Control*, volume 24, 50–62.

Gawronski, W. (2004). *Advanced Structural Dynamics and Active Control of Structures.* Springer.

Gilson, M., Welsh, J.S., and Garnier, H. (2018). A frequency localizing basis function-based IV method for wideband system identification. *IEEE Transactions on Control Systems Technology*, 26(1), 329–335.

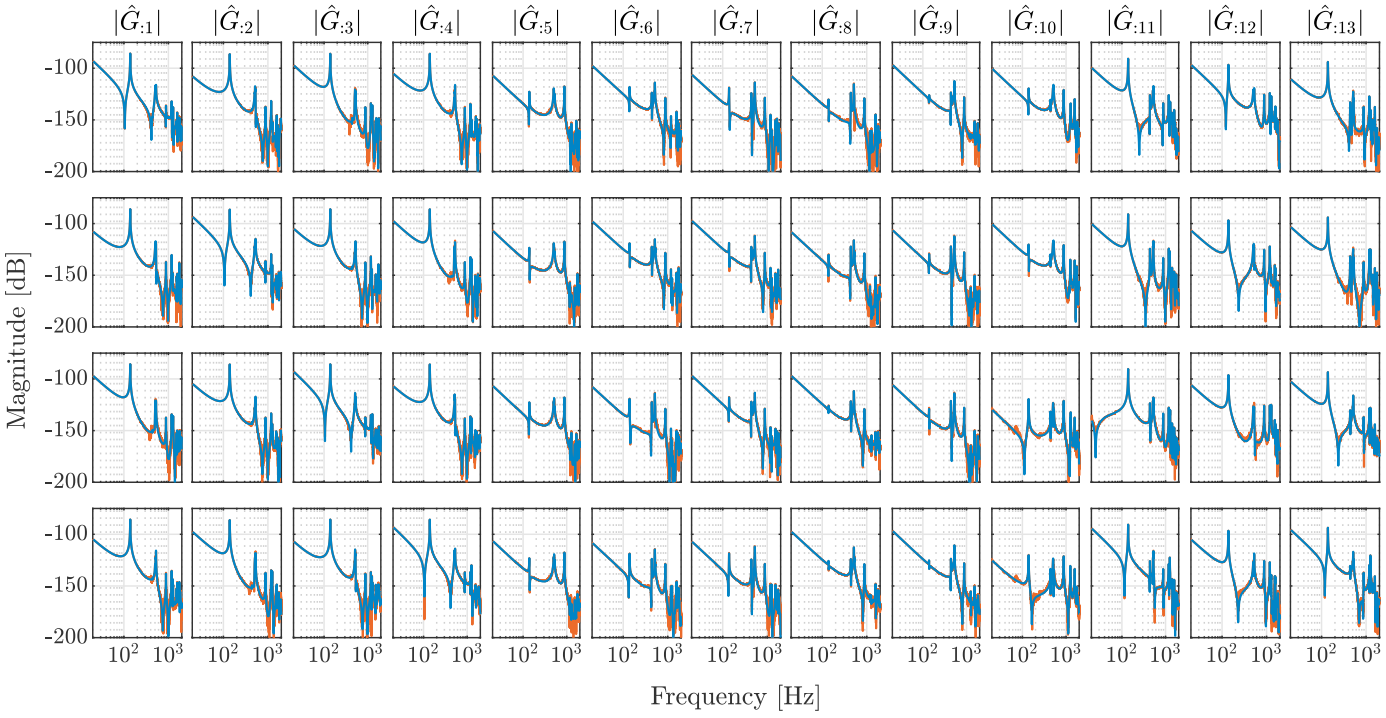

Fig. 4. Element-wise Bode magnitude plot of the FRF measurement (—) and the estimated parametric model (—).

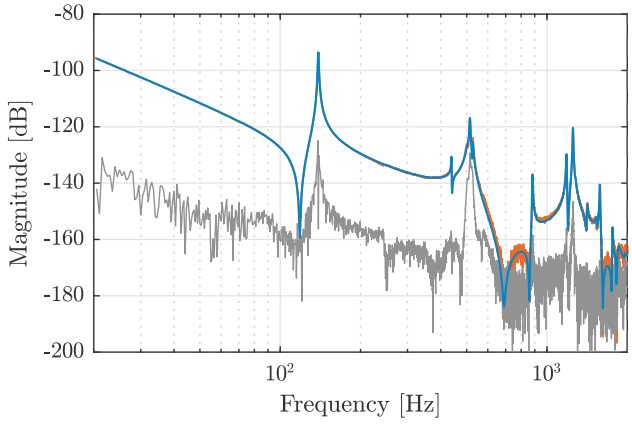

Fig. 5. Bode magnitude plot of the $\hat{G}_{4,13}$ entry with the FRF measurement (—), the estimated parametric model (—) and residual (—).

González, R.A., Classens, K., Rojas, C.R., Welsh, J.S., and Oomen, T. (2024). Identification of additive continuous-time systems in open and closed-loop. *Automatica*, 173(112013).

González, R.A., Rojas, C.R., Pan, S., and Welsh, J.S. (2023). Parsimonious identification of continuous-time systems: A block-coordinate descent approach. In *IFAC World Congress*, 56(2), 4216–4221.

Jian, H.M., Chen, Y.S., and Bai, M.R. (2022). Acoustic modal analysis of room responses from the perspective of state-space balanced realization with application to field interpolation. *The Journal of the Acoustical Society of America*, 152(1), 240–250.

Lange, C. and Leone, M. (2021). Broadband Circuit Model for EMI Analysis of Complex Interconnection Networks in Metallic Enclosures of Arbitrary Shape. *IEEE Transactions on Electromagnetic Compatibility*, 63(2), 474–483.

Ljung, L. (1999). *System Identification: Theory For The User*. Prentice Hall, second edition.

Pintelon, R. and Schoukens, J. (2012). *System Identification*. John Wiley & Sons, New Jersey, second edition.

Sanathanan, C. and Koerner, J. (1961). Transfer function synthesis as a ratio of two complex polynomials. Technical report, Atomic Energy Commission, Ohio.

Semlyen, A. (1999). Rational approximation of frequency domain responses by vector fitting. *IEEE Transactions on Power Delivery*, 14(3).

Shih, C.Y., Tsuei, Y.G., Allemang, R.J., and Brown, D.L. (1988). Complex mode indication function and its applications to spatial domain parameter estimation. Technical Report 4.

Söderström, T. and Stoica, P. (2001). *System Identification*. Prentice Hall.

Steinbuch, M., Oomen, T., and Vermeulen, H. (2022). Motion Control, Mechatronics Design, and Moore's Law. *IEEJ Journal of Industry Applications*, 11(2), 245–255.

Tacx, P., Habraken, R., Witvoet, G., Heertjes, M., and Oomen, T. (2024). Identification of an overactuated deformable mirror system with unmeasured outputs. *Mechatronics*, 99, 103158.

Vayssettes, J. and Mercère, G. (2015). New developments for experimental modal analysis of aircraft structures. In *MATEC Web of Conferences*, volume 20. EDP Sciences.

Vayssettes, J., Mercère, G., and Prot, O. (2016). New developments for matrix fraction descriptions: A fully-parametrised approach. *Automatica*, 66, 15–24.

Voorhoeve, R., De Rozario, R., Aangenent, W., and Oomen, T. (2021). Identifying position-dependent mechanical systems: A modal approach applied to a flexible wafer stage. *IEEE Transactions on Control Systems Technology*, 29(1), 194–206.

Wang, L. and Garnier, H. (2008). *Identification of Continuous-time Models from Sampled Data*. Advances in Industrial Control. Springer London.

Young, P. and Jakeman, A. (1980). Refined instrumental variable methods of recursive time-series analysis. *International Journal of Control*, 31, 741–764.

Zhu, J., Ni, J., and Shih, A.J. (2008). Robust machine tool thermal error modeling through thermal mode concept. *Journal of Manufacturing Science and Engineering*, 130(6), 0610061–0610069.